

Simulation of solidification and convection of $\text{NH}_4\text{Cl-H}_2\text{O}$ solution in a water-cooled copper mold

M. Ahmadein^{1,2,a}, M. Wu^{1,3,b}, M. Stefan Kharicha^{1,c}, A. Kharicha^{1,d},
A. Ludwig^{1,e}

¹ Chair for Modeling and Simulation of Metallurgical Processes, University of Leoben, Austria

² Department of Production Engineering and Mechanical, Tanta University, Egypt

³ Christian-Doppler Laboratory for Advanced Process Simulation of Solidification & Melting, University of Leoben, Austria

^a mahmoud.ahmadein@unileoben.ac.at, ^b menghuai.wu@unileoben.ac.at,

^c mehaela.kharicha@unileoben.ac.at, ^d abdella.kharicha@unileoben.ac.at,

^e andreas.ludwig@unileoben.ac.at

Keywords: modeling, solidification, convection, crystal sedimentation, columnar-to-equiaxed transition, macrosegregation.

Abstract. The convection pattern and the evolution of mushy zone, temperature and solidification structure are measured during solidification of $\text{NH}_4\text{Cl-70}\%\text{H}_2\text{O}$ solution in a water-cooled copper mold with transparent sidewalls. The natural convection and crystal sedimentation are measured via Particle Image Velocimetry (PIV) technique. This experiment is simulated using a 5-phase mixed columnar-equiaxed solidification model proposed by current authors [Comp. Mater. Sci. 50 (2010) 32-42]. The 5 phases comprise the extradendritic melt, the solid dendrite and interdendritic melt inside the equiaxed grains, the solid dendrite and interdendritic melt inside the columnar grains. Melt convection and crystal sedimentation are considered. It is demonstrated that the experimentally observed flow patterns and the solidification structure can be qualitatively reproduced. Reasons for the quantitative deviation between the simulation and experiment are discussed. Analysis of the modeling results in details and improvement of the calculation accuracy will be in a subsequent step.

Introduction

Prediction of the solidification structure is a focal and multifaceted research issue. Incorporating all physical phenomena that influence solidification in one model is very challenging. Simplification of the problem provides a relatively rapid solution with reduced accuracy. However, considering the interacting multi-phase / multi-scale processes during solidification is very costly and increases the model complexity, e.g. transport of heat, momentum, mass, species, and melt and crystal convection. Between the both extremes, several modeling efforts were done by some of the current authors [1-6]. A 5-phase mixed columnar equiaxed solidification model which considered the dendritic morphology was recently suggested [7,8].

A benchmark solidification experiment of $\text{NH}_4\text{Cl-70}\%\text{H}_2\text{O}$ solution was conducted in a $10\times 8\times 1$ cm water-cooled cell with Plexiglas sides [9,10]. Using the Particle Image Velocimetry (PIV) technique and CCD camera, the fluid flow and the solidification process were visualized. An earlier simple 3-phase non-dendritic solidification model [3] was used simulate the benchmark experiment [11]. Some success was achieved to demonstrate the modeling potential for the mixed columnar-equiaxed solidification, but it failed to predict the complex nature of melt flow and crystal sedimentation. In the current work a more advanced 5-phase mixed columnar-equiaxed solidification model [7,8] considering the dendritic morphology is used to reproduce the benchmark experiment numerically.

Model and simulation settings

The model comprises three hydrodynamic phases: liquid melt, equiaxed crystals, and the columnar crystals. The corresponding volume fraction of are f_l , f_e , and f_c . They move with corresponding velocities of \bar{u}_l , \bar{u}_e , and \bar{u}_c . Here \bar{u}_c is predefined as zero which means that the columnar trunks stick to the mold walls. For liquid and equiaxed, \bar{u}_l and \bar{u}_e are solved numerically. Dendritic growth of crystals is taken into consideration. As a result, two additional phase regions exist within each of the equiaxed and the columnar crystal envelopes: the solid dendrites and interdendritic melt. Therefore, five ‘thermodynamic’ phase regions are defined in the system: the solid dendrites and interdendritic melt in the equiaxed grain, the solid dendrites and interdendritic melt in the columnar dendrite trunk, and the extradendritic melt. Each region has correspondingly volume fractions: f_s^e , f_d^e , f_s^c , f_d^c , f_l , and characterized by its corresponding solute concentration: c_s^e , c_d^e , c_s^c , c_d^c , c_l . In order to model the columnar-to-equiaxed transition (CET) both hard blocking [12] and soft blocking [13] mechanisms are considered. A heterogeneous nucleation law with three assumed fitting parameters (ΔT_M , ΔT_σ , n_{max}) [14-16] is used to calculate the nucleation source term for the transport equation of the equiaxed crystals. The melt is assumed to carry initially 10^{+7} m^{-3} of the heterogeneous nucleation sites. For more details about the 5-phase model refer to previous publications [5-8]. The volume averaging approach was employed to formulate the conservation equations of mass, momentum, species, and energy for the assigned phases, in addition to the grain transport equation. The model is implemented in an Eulerian multiphase CFD code (ANSYS Fluent 14.5.0).

A 2D domain being discretized with a grid resolution of 2 mm is shown in Fig.1. A Dirichlet thermal boundary condition is applied for the bottom and side walls according experiment: $T_w = 314.15 - 0.02019 t$, where t is time. T_w is kept constant when it reaches 280.15 K. The calculation starts with following initial conditions: $T_{initial} = 314.15 \text{ K}$, $f_c = 10^{-5}$, $f_e = 10^{-5}$, and the number density of equiaxed crystals of 10^{+5} m^{-3} . The thermo-physical properties of $\text{NH}_4\text{Cl-70\%H}_2\text{O}$ and some modeling parameters are summarized in Table 1. A fixed time step of 10^{-4} s is used for the calculation, and the simulation is terminated at a solidification time of 2000 s. This takes about 18 days using 6 parallel cores (Intel-Sandy-Bridge 2.9 GHz Cluster).

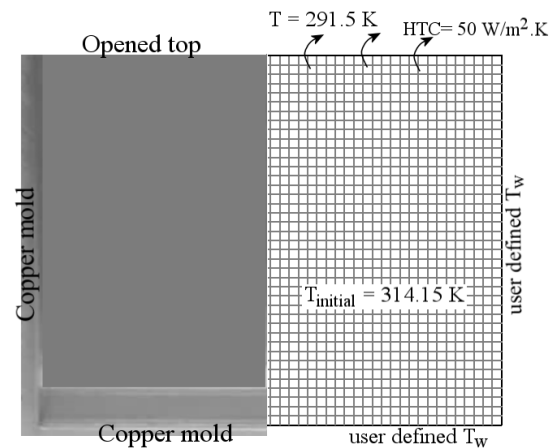


Fig.1. Half of the mold and half of the calculation domain showing the thermal boundary conditions.

Table 1. Thermo-physical properties of $\text{NH}_4\text{Cl-70\%H}_2\text{O}$ and modeling parameters

Liquidus temperature [K]	304.2	Thermal expansion coefficient [K^{-1}]	3.8×10^{-4}
Eutectic temperature [K]	257.2	Solutal expansion coefficient [-]	0.257
Partitioning coefficient [-]	0.0	Primary dendrite arm spacing [mm]	0.6
Slope of liquidus line [K]	- 475	Secondary dendrite arm spacing [mm]	0.1
Diffusion coefficient in liquid [$\text{m}^2 \cdot \text{s}^{-1}$]	2×10^{-9}	KGT growth model:	
Diffusion coefficient in solid [$\text{m}^2 \cdot \text{s}^{-1}$]	8×10^{-13}	K1= 0.0000208136, K2= 0.0000279823	
Latent heat of fusion [$\text{J} \cdot \text{Kg}^{-1}$]	3.1×10^5	Nucleation of equiaxed crystals:	
Density of liquid [$\text{kg} \cdot \text{m}^{-3}$]	1073	$\Delta T_M = 10 \text{ K}$, $\Delta T_\sigma = 3 \text{ K}$, $n_{max} = 10^{+9} \text{ m}^{-3}$	
Density of solid [$\text{kg} \cdot \text{m}^{-3}$]	1102		
Gibbs Thomson coefficient [$\text{K} \cdot \text{m}$]	4×10^{-8}		

Simulation and experiment results

The development of melt convection was tracked during cooling and solidification. A comparison of the velocity fields between the simulation and experiment is shown in Fig.2. Initially, before solidification begins the liquid $\text{NH}_4\text{Cl}-70\%\text{H}_2\text{O}$ solution flows symmetrically with a maximum velocity of ~ 1 mm/s under the effect of thermo-buoyancy as shown in Fig.2a. The cold and denser liquid near the side walls obeys the gravity, whereas the hot bulk rises gently up. As solidification begins, the convection gets stronger and the maximum velocity reaches 1.5 mm/s (Fig.2b). At this stage, a laterally crossing flow coming from the side walls disturbs the up-rising stream in the bulk. The pattern of the flow becomes chaotic and instable. After a while, the lateral flow overwhelms the vertical one and a meandering flow forms as shown in Fig.2c. By analyzing the PIV images similar flow regimes could be distinguished as shown in Fig.2(d-f). The flow starts with a laminar symmetric pattern (Fig.2d), then the disturbed chaotic regime (Fig.2e), followed by a meandering flow (Fig.2f). The order of the maximum velocity measured is very close to that calculated by the numerical model. The meandering flow begins at ~ 22 min, while it was detected at ~ 25 min experimentally.

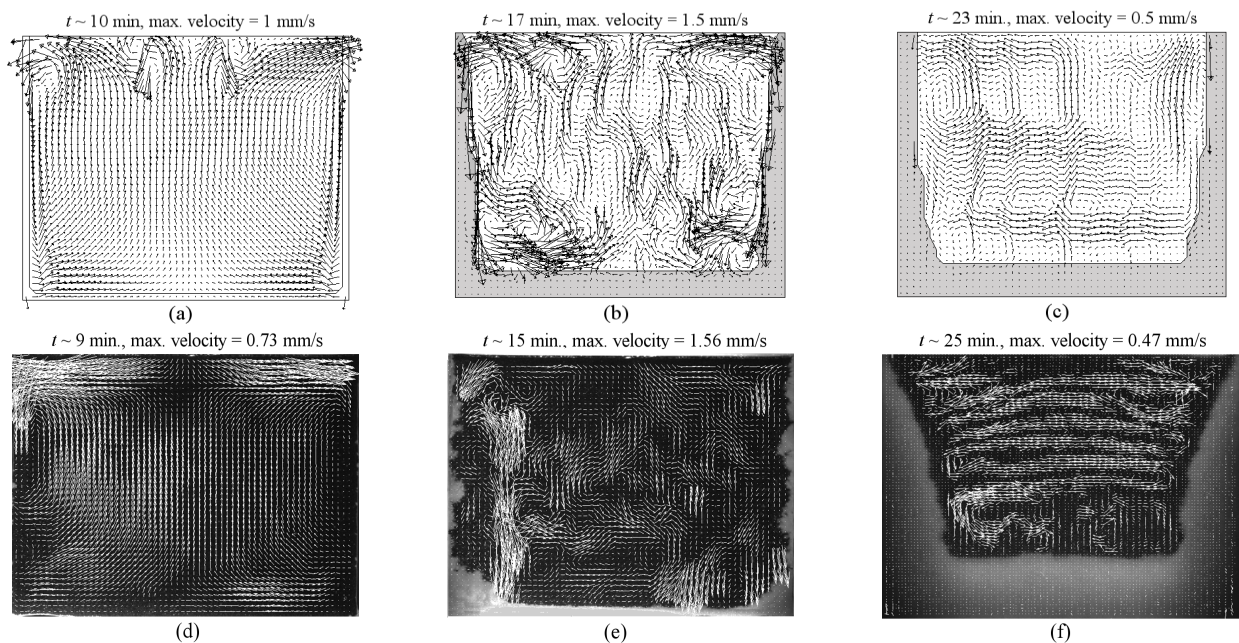


Fig.2. Numerically predicted flow patterns at 3 different stages (a-c), and comparison with the experimentally observed results (d-f). The solid line in simulation represents the solidification front.

The predicted solidification structure was dominantly columnar. Equiaxed growth was unattainable. Demonstratively, some solidification quantities at 23 min are presented in Fig.3.

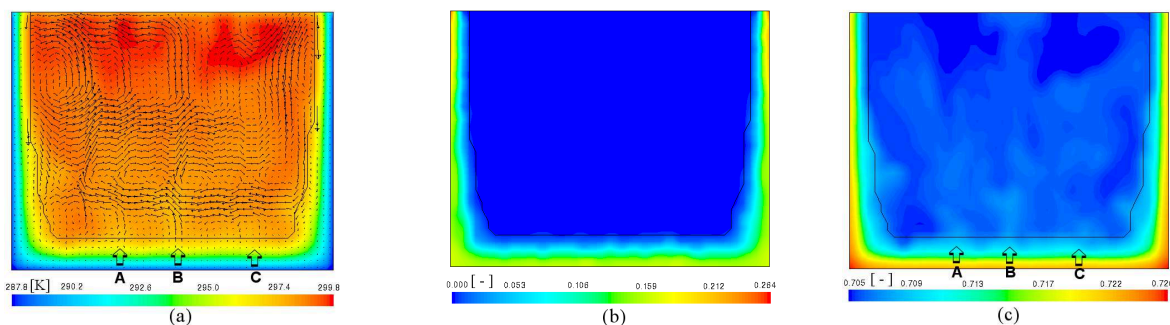


Fig.3. Simulation results at 23 min: (a) liquid temperature superimposed by liquid velocity vectors; (b) volume fraction of columnar; (c) solute (water) concentration in the liquid phase. The solid line represents the solidification front.

The columnar tip front (solid line) separates the bulk liquid region from the mush zone. It is obvious that the temperature profile of liquid in the bulk is somehow disturbed by the flow, whereas a quite uniform temperature gradient develops in the unmoving mush. A gentle interdendritic flow in the mushy zone is still predictable (this is not possibly detected experimentally). Solute (water) enrichment of the interdendritic liquid in the mushy zone can be seen in Fig.3c. The solute-enriched liquid is lighter and tends to rise from the bottom mushy zone. Consequently, plumes form at several locations, e.g. A, B, and C in Fig.3c. The plumes bring the solute-enriched liquid out of the mushy zone, and in the meantime the plumes gently disturb the meandering flow (Fig.3a). Since these plumes are coming from a colder region, the temperature field is also disturbed at the same locations (A, B, and C in Fig.3a)

Experimentally, two different methods were used to analyze the evolution of the mushy zone: (1) the thickness at the center line of the mushy zone in the bottom region, (2) the ratio of integral of mushy zone area to the whole domain, here it is termed as mush fraction. In simulation, both quantities were also monitored, and compared with the experimental results, as shown in Fig.4. Solidification starts at ~ 500 s. After that the thickness of the mushy zone and the mush fraction start to increase. The calculated growth rate of the mush thickness at bottom is initially slower than that of experiment. After ~ 800 s it surpasses that of experiment. At solidification time of 2000 s, the calculated bottom mush is ~ 3 mm thicker than the measured one. The mush fraction increases after 500 s. However, the calculated mush fraction is underestimated compared to the experiment. After ~ 2000 s the calculated and measured mush fraction are very close.

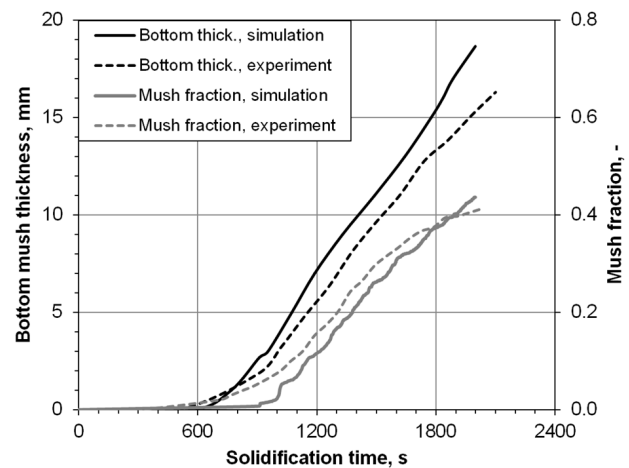


Fig.4. Plots of the calculated and measured thickness of the mushy zone in the bottom region and the so-called mush fraction (ratio of integral of area occupied by the mush to the whole domain).

Discussion

The 5-phase model succeeded to predict the solidification and flow until an advanced solidification time. The results of melt convection agree qualitatively with experiments as shown in Fig.2, where the flow nature alternates from a laminar symmetric to a chaotic instable flow formed by lateral crossing streams, followed by a meandering flow. Quantitatively, both results were also very close. The calculated maximum liquid velocities are very similar to experiment. However, the timing of alteration in flow behavior is slightly different, e.g. the meandering flow in simulation starts at ~ 22 min compared to that in experiment at ~ 25 min. The reason of meandering is not verified yet. According to the present simulation this can be attributed to the response of the thermo-buoyant convective flow at the vertical boundary layer of the dendrite tip front to the interface topography, particularly at the protrusions as shown in Fig.2c. Nevertheless, previous works conducted by some of the current authors using a cellular automaton solidification model revealed similar flow regimes and attributed the meandering flow to the layering of rejected solute [20]. The predicted solutal plumes appeared in Fig.3c also agree with previous numerical and experimental investigations [20,21]. Using a grid 10 times finer than the present one, Kharicha et al. [20] predicted higher number of plumes at the bottom columnar tip front. Further verifications of the influence of grid resolution on the plume formation and the origin of the meandering flow are aimed in the outlook.

Several conditions lead to the quantitative deviation of phase distribution between the simulation and experiment. By comparing the mushy zone in experiment (Fig.2c) and simulation (Fig.3b), the former one has thicker corners and thinner tops. It was observed in the experiment during solidification that some of the crystals formed at the side walls detach, settle down, and accumulate at the bottom corners. The current model assumes that columnar dendrites stick firmly to the wall. Considering crystals detachment lies out of the scope of model improvement at this moment. The overestimation of the mush thickness at the bottom (Fig.4) can be due to growth parameters for the KGT model which are not available for NH_4Cl solution in literature. A future parameter study may be helpful to improve the results. Treating the problem in simulation as 2D can also be a source of quantitative deviation of the results. The thermal boundary condition of the omitted third direction is assumed adiabatic. In experiment the forth and back sides of the mold are bounded by a transparent Plexiglas, which affect the cooling rate of the bulk.

Using the current model settings the predicted solidification structure was dominantly columnar. Experimentally, this structure is irreproducible. Most of trials exhibited columnar growth. However, equiaxed crystals were observed occasionally. Such crystals are carried by the liquid and settle down to form a mixed columnar/equiaxed structure. Detachment and fragmentation of the formed columnar crystals at the mold walls is a probable source for the equiaxed crystals. Additional study is required to verify this issue.

Conclusion

The 5-phase mixed columnar-equiaxed solidification model is able to reproduce the flow behavior and the solidification structure of NH_4Cl -70% H_2O solution. Three flow regimes can be numerically distinguished: an initially formed laminar symmetric flow, a chaotic instable flow formed after solidification, and a meandering flow. Solutal plumes at the bottom columnar tip front can also be predicted. The results agree qualitatively with experiments. The calculated liquid velocity and volume fraction of mush also agree with the experiments. The calculated mush thickness at the bottom and corners deviates slightly from the experiment. Further parameter study and grid verification are suggested to improve the quantitative results of the simulation. Additional efforts have to be done to prove the origin of the accidentally formed equiaxed crystals.

Acknowledgment

This work was financially supported by the FWF Austrian Science Fund (P23155-N24).

References

- [1] T. Wang, S. Yao, X. Zhang, J. Jin, M. Wu, A. Ludwig, B. Pustal, A. Bührig-Polaczek, Modeling of the thermo-solutal convection, shrinkage flow, and grain movement during globular equiaxed solidification in a multi-phase system: I. Three-phase flow model, *Acta Metall. Sinica* 42 (2006) 584-590.
- [2] T. Wang, T. Li, Z. Cao, J. Jin, T. Grimming, A. Bührig-Polaczek, M. Wu, A. Ludwig, Modeling of the thermo-solutal convection, shrinkage flow, and grain movement during globular equiaxed solidification in a multi-phase system: II. Application of model, *Acta Metall. Sinica* 42 (2006) 591-598.
- [3] M. Wu, A. Ludwig, A three-phase model for mixed columnar-equiaxed solidification, *Metall. Mat. Trans. A* 37A (2006) 1613-1631.
- [4] M. Wu, A. Ludwig, Using three-phase deterministic model for the columnar-to-equiaxed transition, *Metall. Mat. Trans. A* 38A (2007) 1465-1475.

- [5] M. Wu, A. Ludwig, Modeling Equiaxed Solidification with Melt Convection and Grain Sedimentation – I: Model Description, *Acta Mater.* 57 (2009) 5621-5631.
- [6] M. Wu, A. Ludwig, Modeling Equiaxed Solidification with Melt Convection and Grain Sedimentation – II: Model Verification, *Acta Mater.* 57 (2009) 5632-5644.
- [7] M. Wu, A. Fjeld and A. Ludwig, Modelling Mixed Columnar-Equiaxed Solidification with Melt Convection and Grain Sedimentation – Part I: Model Description, *Comp. Mater. Sci.* 50 (2010) 32-42.
- [8] M. Wu, A. Ludwig, A. Fjeld, Modelling Mixed Columnar-Equiaxed Solidification with Melt Convection and Grain Sedimentation – Part II: Illustrative Modelling Results and Parameter Studies, *Comp. Mater. Sci.* 50 (2010) 43-58.
- [9] M. Stefan Kharicha, S. Eck, L. Könözy, A. Kharicha, A. Ludwig, Experimental and numerical investigations of NH₄Cl solidification, Part 1: Experimental results, *Int. J. Cast Metal Res.*, 22 (2009) 168-171.
- [10] A. Kharicha, M. Stefan-Kharicha, A. Ludwig, M. Wu, Simultaneous observation of melt flow and motion of equiaxed crystals during solidification using a dual phase particle image velocimetry technique. Part I: stage characterization of melt flow and equiaxed crystal motion, *Metall. Mater. Trans. A* 44 (2013) 650-660.
- [11] L. Könözy, S. Eck, M. Stefan Kharicha, M. Wu, A. Ludwig, Experimental and numerical investigations of NH₄Cl solidification, Part 2: Numerical results, *Int. J. Cast Metal Res.*, 22 (2009) 172-174.
- [12] J. Hunt, Steady-State Columnar and Equiaxed Growth of Dendrites and Eutectic, *Mater. Sci. Eng.* 65 (1984) 75-83.
- [13] M. Martorano, C. Beckermann, Ch-A. Gandin, A solutal interaction mechanism for the columnar-to-equiaxed transition in alloy solidification, *Metall. Mater. Trans. A* 34 (2003) 1657-1674.
- [14] Ph. Thevoz, M. Rappaz, Modeling of Equiaxed Microstructure Formation in Casting, *Metall. Trans. A* 20(1989) 311-322.
- [15] M. Rappaz, Ch.-A. Gandin, Probabilistic Modelling of Microstructure Formation in Solidification Processes, *Acta Metal Mater.* 41 (1993) 345-360.
- [16] M. Ahmadein, B. Pustal, R. Berger, E. Subasic, A. Bührig-Polaczek, Grain nucleation parameters for aluminum alloys: experimental determination and model validation, *Metall. Mater. Trans. A* 40 (2009) 646-653.
- [17] M. Ahmadein, M. Wu, J.H. Li, P. Schumacher, Prediction of the as-cast structure of Al-4.0 Wt. Pct. Cu ingots, A. Ludwig, *Metall. Mater. Trans. A* 44 (2013) 2895–2903.
- [18] C. Beckermann, C.Y. Wang, Equiaxed dendritic solidification with convection: Part III. Comparison with NH₄Cl-H₂O experiments, *Metall. Mat. Trans. A*, 27 (1996) 2784-2795.
- [19] M. Wu, M. Ahmadein, A. Kharicha, A. Ludwig, JH. Li, P. Schumacher, 13th MCWASP, Schladming: Austria, IOP Conf. Ser.: Mater. Sci. Eng., 33, art. no. 012075, 2012.
- [20] A. Kharicha, M Stefan-Kharicha, M. Wu, A. Ludwig, Exploration of the double-diffusive convection during dendritic solidification with a combined volume-averaging and cellular-automaton model, 13th MCWASP, Schladming: Austria, IOP Conf. Ser.: Mater. Sci. Eng., 33, art. no. 012115, 2012.
- [21] C. Beckermann, R. Viskanta, Double-diffusive convection due to melting, *Int. J. Heat Mass Transfer* 31 (1988) 2077-2089.